Fermented Wheat Germ Extract Inhibits Glycolysis/Pentose Cycle Enzymes and Induces Apoptosis through Poly(ADP-ribose) Polymerase Activation in Jurkat T-cell Leukemia Tumor Cells*

Begoña Comín-Anduix‡, László G. Boros‡§, Silvia Marin, Joan Boren, Carles Callol-Massot, Josep J. Centelles, Josep L. Torres¶, Neus Agell‖, Sara Bassilian§, and Marta Cascante**

From the Department of Biochemistry and Molecular Biology, CeRQT-PCB at Barcelona Scientific Park, University of Barcelona, 1 Martí i Franquès, Barcelona 08028, Spain, the §Harbor-UCLA Research and Education Institute, University of California, Los Angeles, School of Medicine, Torrance, California 90502, the ¶Department of Peptide and Protein Chemistry, Institute for Chemical and Environmental Research (IIQAB-CSIC), C/Jordi Girona 18-26, 08034-Barcelona, Spain, and the ‖Department of Cell Biology, IDIBAPS, Faculty of Medicine, University of Barcelona, Casanova 143, E-08036, Barcelona, Spain

The fermented extract of wheat germ, trade name Avemar, is a complex mixture of biologically active molecules with potent anti-metastatic activities in various human malignancies. Here we report the effect of Avemar on Jurkat leukemia cell viability, proliferation, cell cycle distribution, apoptosis, and the activity of key glycolytic/pentose cycle enzymes that control carbon flow for nucleic acid synthesis. The cytotoxic IC_{50} concentration of Avemar for Jurkat tumor cells is 0.2 mg/ml, and increasing doses of the crude powder inhibit Jurkat cell proliferation in a dose-dependent fashion. At concentrations higher than 0.2 mg/ml, Avemar inhibits cell growth by more than 50% (72 h of incubation), which is preceded by the appearance of a sub-G_1 peak on flow histograms at 48 h. Laser scanning cytometry of propidium iodide- and annexin V-stained cells indicated that the growth-inhibiting effect of Avemar was consistent with a strong induction of apoptosis. Inhibition by benzyloxycarbonyl-Val-Ala-Asp fluoromethyl ketone of apoptosis but increased proteolysis of poly(ADP-ribose) indicate caspases mediate the cellular effects of Avemar. Activities of glucose-6-phosphate dehydrogenase and transketolase were inhibited in a dose-dependent fashion, which correlated with decreased ^{13}C incorporation and pentose cycle substrate flow into RNA ribose. This decrease in pentose cycle enzyme activities and carbon flow toward nucleic acid precursor synthesis provide the mechanistic understanding of the cell growth-controlling and apoptosis-inducing effects of fermented wheat germ. Avemar exhibits about a 50-fold higher IC_{50} (10.02 mg/ml) for peripheral blood lymphocytes to induce a biological response, which provides the broad therapeutic window for this supplemental cancer treatment modality with no toxic effects.

The preventive and therapeutic potential of two natural wheat products, wheat bran and fermented wheat germ (Avemar), in experimental carcinogenesis has recently been described (1, 2). Although no chemical constituents are yet isolated and tested experimentally, it is likely that benzoquinones and wheat germ agglutinin in wheat germ and fiber and lipids and phytic acid in wheat bran play a significant role in exerting anti-carcinogenic effects. In a recent report utilizing intracellular carbon flow studies with a ^{13}C-labeled isotope of glucose and biological mass spectrometry (GC/MS),[1] it was demonstrated that the crude powder of fermented wheat germ dose-dependently inhibits nucleic acid ribose synthesis primarily through the nonoxidative steps of the pentose cycle while increasing direct glucose carbon oxidation and acetyl-CoA utilization toward fatty acid synthesis in pancreatic adenocarcinoma cells (3). These metabolic changes indicate that fermented wheat germ exerts its anti-proliferative action through altering metabolic enzyme activities, which primarily control glucose carbon flow toward nucleic acid synthesis.

In vivo, Avemar has a marked inhibitory effect on metastasis formation in tumor-bearing animals (4), and this effect is attributed to its immune-restorative properties (5), which result in a decreased survival time of skin grafts and reduced cell proliferation while enhancing apoptosis. Avemar remarkably inhibits tumor metastasis formation after chemotherapy and surgery in clinically advanced colorectal cancers. Patients receiving standard surgical and chemopreventive therapies for their advanced colorectal cancers developed significantly less new metastases during the 9-month follow-up period when treated with additional 9 g/day Avemar daily (6, 7). In a recent randomized clinical study report Avemar significantly prolonged (doubled) time-to-progression in high-risk melanoma patients (8).

Many anticancer drugs have been shown to induce cell death through the induction of apoptosis. It is well known that apoptosis is a well controlled process by a programmed set of cellular events partially mediated by caspases. A large number of substrates for caspases have been reported, including poly-

‡ Both authors contributed equally to this work.
** To whom correspondence should be addressed: Dept. of Biochemistry and Molecular Biology, IDIBAPS, University of Barcelona, 1 Martí i Franquès, Barcelona 08028, Spain. Tel.: 34-934021593; Fax: 34-934021219; E-mail: marta@bq.ub.es.

[1] The abbreviations used are: GC/MS, gas chromatography/mass spectrometry; FACS, fluorescence-activated cell sorting; G6PDH, glucose-6-phosphate dehydrogenase; HK, hexokinase; LDH, lactate dehydrogenase; LSC, laser-scanning cytometry; FC, flow cytometry; PBL, peripheral blood lymphocytes; PI, propidium iodide; Z-VAD.fmk, benzyloxycarbonyl-VAD-fluoromethyl ketone; FITC, fluorescein isothiocyanate; PARP, poly(ADP-ribose) polymerase; IDIBAPS, Institute Investigations Biomediques August Pi I Sunyer.

(ADP-ribose) polymerase (PARP), a 116-kDa nuclear DNA repair enzyme that is cleaved during apoptosis by caspases-3 and -7 (9, 10). Powerful and selective reversible and irreversible peptide-based inhibitors are also available to better characterize and understand the mechanism(s) of how caspases regulate apoptosis. The tripeptide benzyloxycarbonyl-Val-Ala-Asp fluoromethyl ketone (Z-VAD.fmk) is a broadly used general caspase inhibitor that blocks apoptosis in many cell types, including human leukemic Jurkat T cells (10, 11).

Here we report the effect of fermented wheat germ on cell cycle regulation, proliferation, and apoptosis induction in Jurkat leukemia cell cultures. Our results confirm strong tumor growth inhibitory properties of Avemar and additionally reveal its cell cycle-regulating characteristics. Avemar decreases G6PDH and transketolase activities that are key enzymes involved in glucose conversion into the five-carbon nucleotide precursor ribose pool. Stable isotope studies indicate that Avemar is a powerful inhibitor of *de novo* nucleic acid synthesis. This likely is the underlying mechanism of the anti-proliferative tumor growth-controlling and apoptosis-inducing potential of fermented wheat germ in leukemia tumor cells. On the contrary, Avemar has no toxic biological effects on PBLs in the doses that affect tumor cells in an adverse manner.

MATERIALS AND METHODS

Chemicals—Ribose 5-phosphate, xylulose 5-phosphate, $MgCl_2$, triose-phosphate isomerase, NADH, thiamine pyrophosphate (TPP), glucose 6-phosphate, dithiothreitol, $NADP^+$, propidium iodide (PI), Igepal CA-630, Ponceau S, and vincristine were purchased from Sigma Co. and Tris from ICN Pharmaceuticals Inc (Costa Mesa, CA). The Bio-Rad protein assay was purchased from Bio-Rad and the BCA protein assay from Pierce. Fetal bovine serum, RPMI 1600 medium was purchased from Invitrogen (Carlsbad, CA). Dulbecco's phosphate-buffered saline (PBS), typsin-EDTA and solution C (0.05% trypsin and EDTA (1:500) in PBS) were purchased from Biological Industries (Kibbutz Beit Haemek, Israel). Nitrocellulose strips were purchased from Schleicher & Schuell (Postach, Dasell, Germany). Annexin V was purchased from Bender MedSystems (Vienna, Austria), PARP from BD PharMingen cat. 66391 A and clone 7D3-6) and the secondary antibody anti-mouse immunoglobulin from DAKO (Copenhagen, Denmark). ECL was purchased from Amersham Biosciences. FK-109 Z-VAD.fmk were from Enzyme Sysytems Products (Livermore, CA). Avemar was kindly provided by Biromedicina, Co. (Budapest, Hungary) through a material and chemical transfer agreement.

Cell Culture—Jurkat cells (acute lymphoid T-cell leukemia) were purchased from ATCC and cultured in RPMI 1640 medium supplemented with 10% (v/v) heat-inactivated fetal calf serum, 2 mM L-glutamine, and antibiotics: 100 units/ml penicillin and 100 μg/ml streptomycin (Invitrogen). Cells were grown in an isolated 37 °C, 5% CO_2 tissue incubator compartment. Cells were plated in $0.2–1 \times 10^5$ cells/ml density for the enzyme kinetics experiments in T75 culture flasks. For apoptosis, necrosis, and cell cycle studies cells were seeded into 6-well plates at 5×10^5 cells/well density. Avemar was added to the cultures after 1 h of equilibration in the cell culture chambers after seeding. Avemar was dissolved in Dulbecco's PBS for all experiments. Control cultures were treated with an equal volume of PBS as the Avemar-treated cultures. Jurkat cell cultures used in this study were free of mycoplasm infection as shown by the Gen-probe rapid mycoplasm detection system prior to treatments with Avemar. Peripheral blood mononuclear cells from healthy donors were isolated from buffy coat cells using the Ficoll gradient method (12); further purification of lymphocytes from peripheral blood mononuclear cells was performed by depletion of contaminating cells by adherence to plastic plates for 4 h. PBL were used as non-dividing and non-tumor cells to test the apoptosis-inducing effects of Avemar in a control cell system.

Cell Cycle Analysis—Jurkat cells were harvested after Avemar treatment and stained in Tris-(hydroxymethyl)aminomethane-buffered saline containing PI (50 μg/ml), ribonuclease A (10 μg/ml), and Igepal CA-630 (0.1%) for 1 h at 4 °C. DNA content was analyzed by fluorescence-activated cell sorting (FACS). Fluorescence of 12,000 Jurkat cells was acquired for each histogram and then analyzed using the Multicycle program interface (Phoenix Flow Systems, San Diego, CA). Flow cytometry DNA histograms were collected in triplicates on an XL flow cytometer (Coulter Corporation, Hialeah, FL).
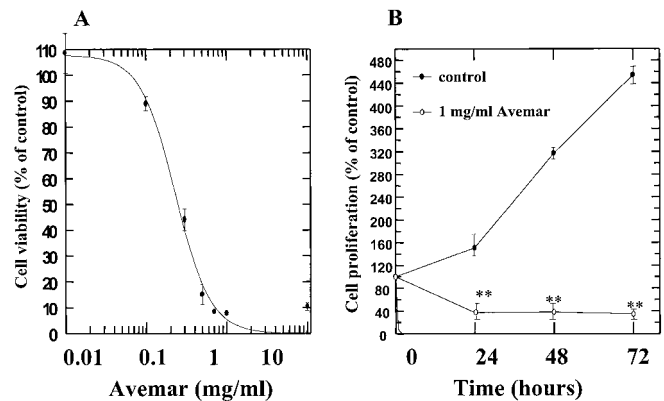

FIG. 1. **Jurkat leukemia cell proliferation in response to Avemar treatment.** Jurkat cell cultures were treated with increasing doses of Avemar as indicated on the *x* axis; their viability and proliferation were determined by formazan dye uptake and expressed as percent of untreated control cell proliferation (*A*). 1 mg/ml Avemar inhibited cell proliferation in a time course study of up to 72 h in culture (*B*). Mean ± S.D., $n = 9$; *, $p < 0.05$; **, $p < 0.01$.

Cell Viability Assay—Cell number was determined by the MTT (3-(4,5-dimethylthiazol-2-yl)-2,5-diphenyltetrazolium bromide) assay (13). 20,000 Jurkat cells per well were incubated in 96-well plates in the presence or in the absence of Avemar at different concentrations. Vincristine was used as a positive control for apoptosis induction. The blue MTT formazan precipitate was dissolved in 100 μl of Me_2SO, and the absorbance values at 550 nm were determined on a multiwell plate reader. For peripheral blood cells, 500,000 cells were seeded in 12-well plates in the presence or in the absence of Avemar at different concentrations. Viability was estimated by a MultiziserIIL Coulter (Beckman Coulter, Fullerton, CA) to count the cells and by FACS analysis adding 18 μg/ml PI (Sigma Co.) staining method without cell permeabilization. The fluorescence of cells was analyzed by flow cytometry using an Epics XL flow cytometers (Beckman Coulter, Fullerton, CA). Only non-viable cells are PI positives as indicated by previous studies (14).

Assessment of Apoptosis by Flow Cytometry and LSC—Jurkat cells after Avemar treatment were washed once in binding buffer (10 mM HEPES, sodium hydroxide, pH 7.4, 140 mM sodium chloride, 2.5 mM calcium chloride) and resuspended in the same buffer at 10^6 cells ml^{-1} in the presence of 0.5 μl of annexin V-FITC. After 30 min of incubation at room temperature, PI was added at 0.05 μg ml^{-1} (11). The fluorescence of cells was analyzed by FC and LSC. Approximately 3×10^4 cells were tested for each histogram for FC and 1500 cells for LSC.

Gel Electrophoresis and Immunoblotting of PARP—To analyze PARP, SDS-page electrophoresis (15) and immunoblotting were performed as previously described (16). Briefly, 30 μg of the protein extract was used on an 8% polyacrylamide gel and transferred to Protean membranes (Schleicher & Schuell, GmbH, Postach, Dasell, Germany). Monoclonal antibodies either against PARP were used at a 1:1000 dilution. As a control of protein loading the blot membrane was stained with Red Ponceau. The reaction was visualized with a secondary antibody (anti-mouse immunoglobulin, DAKO) conjugated to horseradish peroxidase diluted 1:1000 in bovine serum albumin/Tween-20/PBS and the enhanced chemiluminescence (ECL) detection kit (Amersham Biosciences). PARP immunoblotting was performed after 48 h of incubation with the Avemar and vincristine. The protein concentration of cell extracts was determined by the BCA protein assay.

Measurements of Enzyme Activities—Jurkat cells treated with increasing doses of Avemar were lysed in 1 ml of 20 mM Tris buffer (pH 7.5) containing 1 mM dithioerythreitol and 0.2 mM phenylmethylsulfonyl fluoride, 1 mM K-EDTA, 0.2 g/liter Triton X-100, and 0.2 g/liter sodium deoxycholate. Cell extracts were stored at −20 °C for 24 h. The homogenates were then defrosted in an ice bath, sonicated in a Brason–2000 cell disintegrator for 5 min, ultracentrifuged at $100,000 \times g$ for 1 h, and the supernatant used for enzyme activity assays as described below.

Transketolase (EC 2.2.1.1) activity was determined using the enzyme-linked method of De La Haba *et al.* (17). 1-ml aliquots of transketolase free buffer were measured in spectrophotometry cuvettes containing 50 mM Tris-HCl, pH 7.6, 2 mM ribose 5-phosphate, 1 mM xylulose 5-phosphate, 5 mM $MgCl_2$, 0.2 units/ml triose-phosphate isomerase/α-glyceraldehyde-3-phosphate dehydrogenase, 0.2 mM NADH, and 0.1 mM thiamine pyrophosphate. The transketolase reac-

Tumor Cell Apoptosis Induced by Fermented Wheat Germ Extract

tion was initiated by the addition of 25 and 50 μl of cell extract at 37 °C. The oxidation of NADH, which is directly proportional to transketolase activity, was measured by the decrease in 340-nm absorbance. Transketolase activity is expressed as nmol/min/million cells.

Glucose-6-phosphate dehydrogenase (G6PDH; EC 1.1.1.49) activity was measured as described by Tian *et al.* (18). Briefly, cuvettes were prepared with a 50 mM Tris-HCl, pH 7.6 buffer, containing 2 mM glucose 6-phosphate and 0.5 mM NADP$^+$. Reactions were initiated by the addition of 25 and 50 μl of cell extract at 37 °C. The reduction of NADP, which is directly proportional to G6PDH activity, was quantified by the increase in 340-nm absorbance, and G6PDH activity is expressed as nmol/min/million cells.

Lactate dehydrogenase (LDH; EC 1.1.1.27) activity was measured as described by Mommsen *et al.* (19). The assay medium for lactate dehydrogenase contained 50 mM Tris-HCl buffer, pH 7.6, 0.2 mM NADH, and 5 mM pyruvate (omitted for control). The oxidation of NADH, which is directly proportional to lactate dehydrogenase activity, was measured by the decrease in 340-nm absorbance. LDH activity is expressed as nmol/min/million cells.

Hexokinase (HK; EC 2.7.1.1) activity was measured by the enzyme-linked method of Grossbard and Schimke (20). Briefly, cuvettes were prepared with a 50 mM Tris-HCl, pH 7.6 buffer, containing 10 mM glucose, 1 mM NADP$^+$, 2 mM ATP, 10 mM magnesium chloride, and 1 unit of G6PDH. Reactions were initiated by the addition of 50 and 100 μl of cell extract at 37 °C. The reduction of NADP, which is directly proportional to HK activity, was quantified by the increase in 340-nm absorbance, and HK activity is expressed as nmol/min/million cells.

Stable Isotope Incorporation into RNA Ribose—In order to measure actual substrate carbon flow in the pentose cycle and glycolysis, which are controlled by the enzymes listed above, we utilized stable isotope-based metabolic profiling as introduced for drug effect studies in cancer (21). Jurkat cell continuous S phase-independent nucleic acid synthesis rates were measured by the incorporation of $[1,2\text{-}^{13}C_2]$glucose into RNA ribose as the single tracer and biological mass spectrometry. ^{13}C label accumulation into RNA was determined by measuring the molar enrichment (ME) of ribose using chemical ionization methods, which is capable of determining both total activity (Σm_n) and positional distribution of ^{13}C labels in nucleic acid ribose as described previously (22, 23).

Stable Isotope Incorporation into Lactate—Lactate from the cell culture media (0.2 ml) was extracted by ethyl acetate and derivatized to its propylamine-HFB form. The *m/z* 328 (carbons 1–3 of lactate, chemical ionization) ion cluster was monitored for the detection of *m1* (recycled lactate through the pentose cycle) and *m2* (lactate produced by glycolysis) for the estimation of the pentose cycle activity relative to glycolysis (23).

Gas Chromatography/Mass Spectrometry—Mass spectral data were obtained on the HP5973 mass selective detector connected to an HP6890 gas chromatograph. The settings were as follows: GC inlet, 230 °C; transfer line, 280 °C; MS source, 230 °C; MS Quad, 150 °C. An HP-5 capillary column (30-m length, 250-μm diameter, 0.25-μm film thickness, Supelco) was used for ribose analysis at the ion cluster *m/z* 256 and for lactate analysis (23).

Data Analysis and Statistical Methods—Experiments *in vitro* were carried out using three cultures each time for each treatment regimen and then repeated twice. Mass spectral analyses were carried out by three independent automatic injections of 1-μl samples by the automatic sampler and accepted only if the standard sample deviation was less than 1% of the normalized peak intensity. Enzyme activity measurements were determined after correction for total protein content in cell extracts. Statistical analysis was performed using the parametric unpaired, two-tailed independent sample Student's *t* test with 99% confidence intervals ($\mu \pm 2.58\sigma$) and $p < 0.01$ was considered to indicate significant differences in glucose carbon metabolism and enzyme activities with increasing doses of Avemar. Because of the human cell line involved, a clearance was obtained from the Institutional Review Boards (IRB) of both Harbor-UCLA and The University of Barcelona for the use of these commercially available cells for the experiments reported.

RESULTS

For the present report, Jurkat lymphoid T- cell leukemia cells were treated with increasing amounts of Avemar for either 48 or 72 h in order to estimate the growth regulating effects of this natural anti-cancer nutritional supplement through cell cycle modulation, apoptosis induction, metabolic enzyme activity changes as well as substrate flow measure-
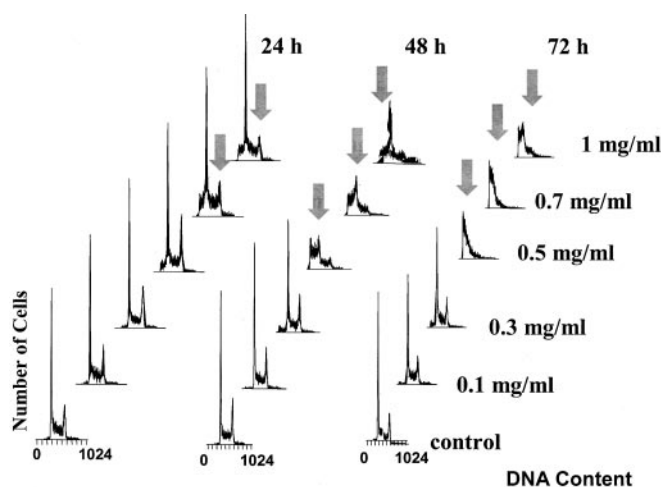

FIG. 2. **Jurkat leukemia cell cycle changes in response to Avemar treatment.** Jurkat cell cultures were treated with increasing doses of Avemar as indicated on the *right column*, and cell cycle distribution was determined using flow cytometry after PI staining expressed as percent of G_0/G_1, S, and G_2-M cycle phases. The DNA *histograms* show that Avemar induced a time- and dose-dependent decrease in the S cycle phase whereas there was a significant expansion of the G_0/G_1 cycle phase consistent with an increase in the number of apoptotic Jurkat cell figures. The typical FACS analysis showed the distinct signals and cell frequencies associated with the arrested cell cycle status as described under "Results" ($n = 6$).

ments. Avemar doses of 10 mg/ml (stock) and its serial dilutions were selected for the study because the effective oral dose of Avemar that inhibits tumor metastasis formation is 9.0 g/day, which is equivalent to an estimated plasma concentration of 0.5 and 1 mg/ml in an average (70 kg) weight patient (6).

Cytotoxic Effects of Avemar on Jurkat cells—Avemar induced a dose-dependent decrease in vital formazan dye accumulating cells after 72 h of treatment, ranging from 0 to 10 mg/ml (Fig. 1*A*). The mean IC$_{50}$ of Avemar was 0.23 ± 0.03 mg/ml. The cytotoxicity of Avemar on Jurkat cells was studied using a time course experiment. A significant increase in cell death by formazan exclusion was detected as early as 24 h with 1 mg/ml Avemar treatment (Fig. 1*B*). The mean IC$_{50}$ of vincristine as a positive control was 0.18 ± 0.02 nM. Avemar exhibited about 50-fold higher IC$_{50}$ (10.02 mg/ml) for PBLs to induce biological responses.

Cell Cycle—In control cultures the cell cycle pattern remained constant over time; the percentage of cells in the G_0/G_1 phase: 40, 39, and 42%; S phase: 35, 39, and 34%; and G_2/M phase: 25, 23, and 23% after 24, 48, and 72 h, respectively (Fig. 2). A complete alteration of the cell cycle patterns became evident as shown in Fig. 2 by the *gray arrows* after 48 and 72 h with 0.5 mg/ml or higher Avemar concentrations. At concentrations of 0.7 and 1 mg/ml Avemar, even after 24 h, a broad peak appeared in the sub-G_1 region with a significant decrease in the S cycle phase. The sub-G_1 region is indicative of apoptosis (Fig. 2, *black arrows*). Although lower concentrations of Avemar (0.1 and 0.3 mg/ml) induced only minor changes in the cell cycle distribution of Jurkat cells, they were still effective in controlling cell growth as there was a significant decrease in formazan-accumulating Jurkat cells as shown in Fig. 1*A*.

Induction of Apoptosis—Avemar triggered prominent apoptosis at 0.5 mg/ml dose after 72 h of culturing as demonstrated by FACS analysis. Increasing doses of Avemar induced more prominent apoptosis, which also appeared earlier (Fig. 3*A*). In order to discriminate between late apoptotic and necrotic cells, we investigated PI and annexin V-FITC positive cells using LSC analyses. We observed that all cells with PI$^+$/FITC$^+$ char-
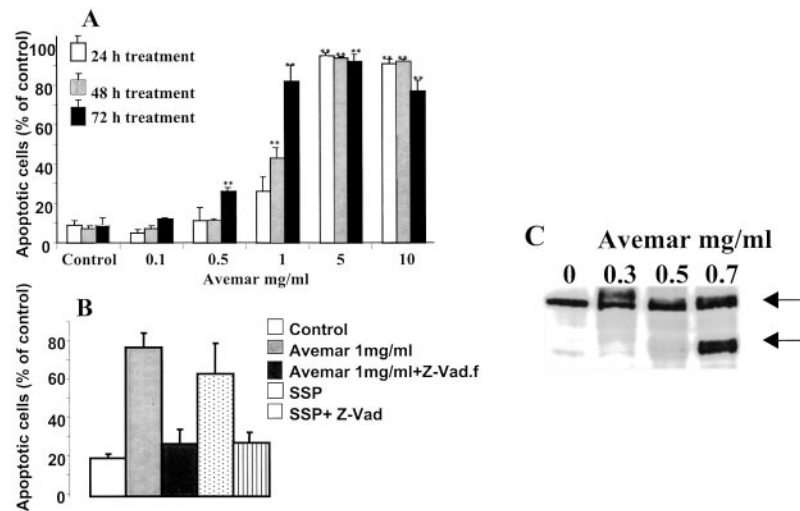
FIG. 3. **Jurkat leukemia cell apoptosis in response to Avemar treatment.** *A*, Jurkat cell cultures were treated with increasing doses of Avemar as indicated on the *x* axis, and the number of apoptotic Jurkat cell was determined using flow cytometry after PI and annexin V staining. 24-hour treatment is shown with *open bars*, 48-h treatment with *light gray bars,* and 72-h treatment with *dark gray bars*. It can be depicted that Avemar induced a time- and dose-dependent increase in apoptosis in Jurkat cells in culture. Time dependence is clear at the 0.5 and 1 mg/ml dose treatments. Mean $\pm$ S.D., $n = 9$; *, $p < 0.05$; **, $p < 0.01$. *B*, percentage of annexin V positive cells after 72 h of treatment with and without the caspase inhibitor Z-VAD.fmk (100 μM) of Avemar-treated cultures (1 mg/ml). Mean $\pm$ S.D., $n = 5$; **, $p < 0.01$. Positive controls were treated with 1 μM of staurosporin (*SSP*). *C*, Western blots of extracts prepared from cells treated for 48 h with the indicated concentrations of Avemar (0 control; 0.3, 0.5, or 0.7 mg/ml) and probed with anti-PARP antibody. The position of native PARP (116 kDa) and the proteolytic fragment (85 kDa) is indicated here.

acteristics presented pycnotic nuclei, which is a definite sign of apoptotic cell formation after treatment with 1 mg/ml Avemar (72 h). The portion of normal cell figures with LSC was only 5.5%, whereas early apoptotic cells showed 64.5% and late apoptotic cells 29.3% frequency (Fig. 4). All Avemar-treated Jurkat cells inside the PI$^-$/FITC$^+$ region presented the typical green appearance of early apoptosis caused by the labeling of annexin V by FITC.

Involvement of Caspases in the Apoptotic Effect of AVE-MAR—Decreased apoptosis-related phosphatidylserine externalization by specific caspase inhibitors is a routinely used method to reveal the presence of caspase cascades in the cell death process. In order to assess the involvement of caspases in the apoptotic effect of Avemar, we studied whether the caspase inhibitor Z-VAD.fmk could prevent Avemar-induced phosphatidylserine externalization. Jurkat cells incubated for 72 h with 1 mg/ml of Avemar in the presence or absence of 100 μM Z-VAD.fmk showed severely decreased phosphatidylserine externalization in both early (annexin V-FTIC$^+$/PI$^-$) and late (annexin V-FTIC$^+$/PI$^+$) apoptotic cells (Fig. 3*B*).

We also investigated whether incubation of Jurkat cells with different doses of Avemar induced proteolytic cleavage of PARP, which is considered to be a hallmark of activation of caspase-3 like proteases during apoptosis (24, 25). Incubation of Jurkat cells for 48 h with 0, 0.3, 0.5, and 0.7 mg/ml of Avemar induced prominent cleavage of PARP at a concentration of 0.5 mg/ml or higher (Fig. 3*C*).

Transketolase and G6PDH Enzyme Activities—G6PDH and transketolase are two key enzymes that regulate carbon flow in the pentose cycle because of their high substrate flux coefficients and thus regulate ribose synthesis and NADPH production for proliferating cells (24–26). Avemar inhibited G6PDH activity at concentrations of 0.7 mg/ml and higher after 48 h of treatment, and G6PDH was completely inhibited after 72 h (Fig. 5*A*). Transketolase was significantly inhibited with 0.7 and 1 mg/ml Avemar after 72 h of treatment (Fig. 5*B*).

HK and LDH Enzyme Activities—HK and LDH are two of the key enzyme in the regulation of glycolytic flux. Avemar inhibited LDH and HK at concentrations of 0.3 mg/ml or higher after 48 h of treatment as shown on Fig. 6.
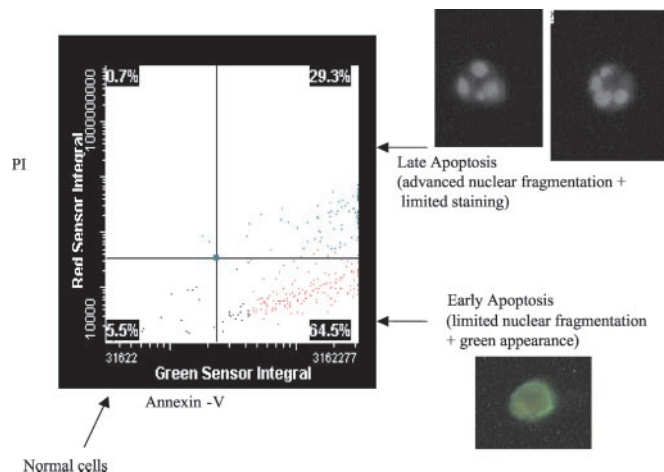

FIG. 4. **Jurkat leukemia cell apoptosis and necrosis in response to Avemar treatment using LSC.** Jurkat cell cultures were treated with 1 mg/ml Avemar (72 h), and the formation of apoptotic and necrotic Jurkat cell figures was determined using PI and Annexin V-FITC staining. The majority (64.5%, *right bottom quadrant*) of Jurkat cells exhibited early apoptosis as indicated by the limited nuclear fragmentation. Late apoptosis/necrosis was present in about 30% (*right upper quadrant*) of Jurkat cells with advanced nuclear fragmentation and limited staining, while the frequency of normal cells dropped to 5.5% as seen in the *left bottom quadrant* of the LSC screen ($n = 6$).

[13]C Label Accumulation in Lactate—We observed a decrease in *m2* and *m1* [13]C label in lactate in Avemar-treated Jurkat cells, which is indicative of decreased glucose uptake and glycolysis. Overall carbon flux in the pentose cycle relative to glycolysis showed a dose-dependent non-significant increase in Jurkat cells after 2 days of Avemar treatment after 0.1 and 0.5 mg/ml treatments. At the dose of 1 mg/ml Avemar treatment the pentose cycle showed a rapid 22% decrease relative to glycolysis, as indicated by decreased *m1/m2* [13]C ratios in lactate (Table I).

[13]C Label Accumulation in RNA Ribose—In order to estimate nucleic acid precursor synthesis measurements of the molar enrichment of RNA ribose with ^{13}C from glucose was
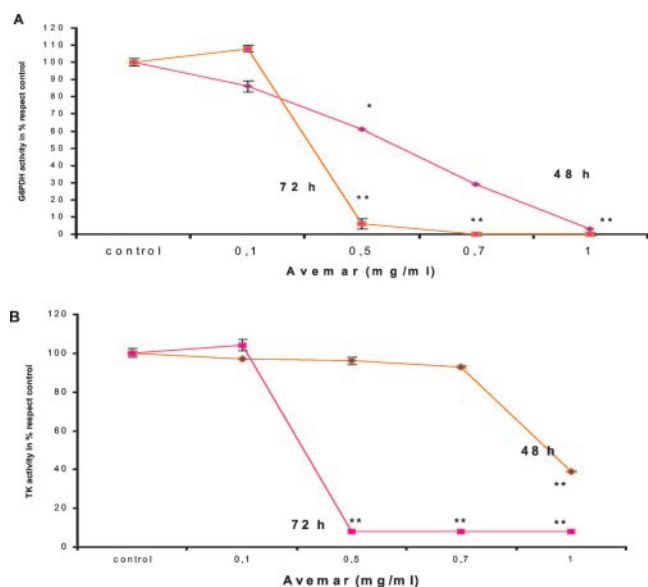
FIG. 5. **Jurkat leukemia cell G6PDH (*A*) and transketolase (*B*) enzyme activities in response to 48 and 72 h of Avemar treatment.** Avemar inhibited both G6PD and transketolase in a dose- and time-dependent manner. Mean $\pm$ S.E.; $n = 9$; *, $p < 0.05$; **, $p < 0.01$.
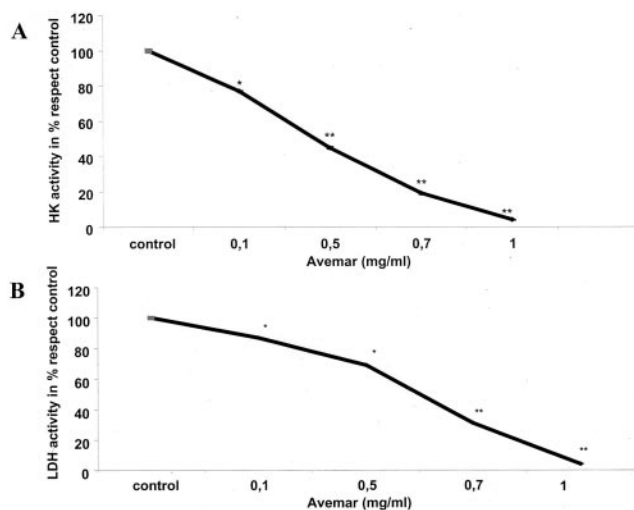

FIG. 6. **Jurkat leukemia cell hexokinase (*A*) and lactate dehydrogenase (*B*) enzyme activities in response to 48 h of Avemar treatment.** Avemar inhibited both enzymes in Jurkat cells in a dose-dependent manner. Mean $\pm$ S.E., $n = 14$; *, $p < 0.05$; **, $p < 0.01$.

carried out because ribosomal and messenger RNAs are continuously synthesized in tumor cells regardless of their proliferative response, cell cycle alterations and apoptosis formation in response to anti-carcinogenic treatments. [13]C incorporation from glucose into RNA ribose was significantly and dose-dependently decreased after increasing doses of Avemar treatment (Table II). Increasing doses of Avemar (0.1, 0.5, 1 mg/ml) decreased glucose carbon incorporation into nucleic acid synthesis by 6, 20.4, and 40.2%, respectively, after 48 h of incubation, which correlated well with the decrease in G6PDH and transketolase activities (Figs. 5 and 6).

DISCUSSION

Because of their beneficial nutritional values, wheat germ and wheat bran are frequently used in human food supplements, breakfast cereals, nutri-bars, and various fiber drink mixtures; therefore, they are part of the regular Western diet. Avemar is the first fermented and concentrated wheat germ extract produced by an optimized process to yield 0.4 mg/g (on

dry matter basis) 2,6-dimethoxy-*p*-benzoquinone and given as a nutritional supplement for cancer patients. The suspicion that wheat germ contains powerful cancer-fighting chemicals is not new; in his later life, the Nobel laureate biochemist Albert Szent-Györgyi studied various extracts of the wheat plant extensively for their anti-carcinogenic effects.

This study investigates the complex responses to Avemar treatment, a potent natural fermented wheat germ extract with anticarcinogenic properties, of Jurkat T-progeny leukemia cells in culture. Using flow and laser scanning cytometry techniques, direct enzyme activity measurements, carbon substrate flow measurements with a ^{13}C-labeled glucose tracer has enabled us to study a broad range of cellular response mechanisms, such as cell cycle progression, apoptosis, cell proliferation, and their dose-response to this cancer growth-modifying agent. Activity changes of four important metabolic enzymes involved in direct glucose oxidation (G6PDH), non-oxidative glucose utilization (transketolase) toward nucleic acid synthesis, glycolysis (LDH), and glucose activation (HK) are herein also reported. Our studies revealed profound differences and a dose-dependent response of Jurkat leukemia cells that directly affected metabolic enzyme activities, metabolic pathway substrate flow, apoptosis formation, and cell proliferation in response to Avemar. It has previously observed that G6PDH inhibition leads to an increase in apoptosis formation in tumor cells of various origins (26, 27). In contrast, Avemar treatment according to our results is about $50\times$ less effective in peripheral blood lymphocytes in inducing biological effects, which provides a comfortable therapeutic window for Avemar to apply in patients as a supplemental treatment modality with minimal or no toxic side effects.

It has been proved that the flip-flop of phosphatidylserine from the inner to the outer plasma membrane leaflet of the cell is a fundamental characteristic that differentiates apoptosis from necrosis (28). This early phenomenon during the apoptotic process is followed by caspase activation, which can specifically be inhibited and the fact that this inhibitor effectively inhibited Avemar-induced phosphatidylserine externalization demonstrated the involvement of caspases in mediating the biological apoptosis-inducing effects of Avemar. Furthermore, we detected a cleavage of PARP during Avemar-induced apoptosis in Jurkat cells, which more specifically points to the involvement of caspase-3 in the cascade that mediates wheat germ-induced apoptosis. Based on these molecular findings our data also indicate that the mechanism of how Avemar mitigates metastasis also involves decreasing cell motility.

It has recently been demonstrated that Avemar induces profound metabolic changes in cultured MIA pancreatic adenocarcinoma cells using the $[1,2\text{-}^{13}C_2]$glucose isotope as the single tracer and biological gas chromatography/mass spectrometry. It was concluded that Avemar controls tumor propagation primarily through the regulation of glucose carbon redistribution between cell proliferation- and cell differentiation-related macromolecules in MIA cells (3). In the present study we again applied stable isotope-based dynamic metabolic profiling as a model for measuring metabolic pathway control characteristics (29) by demonstrating a dose-dependent decrease in substrate carbon flow toward nucleic acid precursor ribose synthesis and metabolic enzyme activities (G6PDH, transketolase, HK, and LDH) in Jurkat leukemia cells treated with comparable doses of Avemar. Indeed, Jurkat cells also responded with decreased carbon flow through the pentose cycle toward nucleic acid synthesis and in this study the significant, dose-dependent decrease of G6PDH and transketolase are also demonstrated. It is likely that decreased oxidative ribose synthesis in response to Avemar treatment in Jurkat cells is not able to supply the

TABLE I
Lactate production of Jurkat cells in response to increasing doses of Avemar treatment after 48 h of culture

Lactate isotopomers derive from $[1,2\text{-}^{13}C_2]$glucose based on glycolysis (*m2*) or direct glucose oxidation (*m1*). PC represents the pentose cycle, and it is defined as a percentage of direct glucose oxidation/recycling of the glycolytic flux or *m1/m2* ratios in the released lactate into the culture media.

Lactate	m0	m1	m2	m1/m2	PC
Control	0.809	0.006	0.1849	0.0322	1.06%
Avemar					
0.1 mg/ml	0.8211	0.0062	0.1723	0.0359	1.18%
0.5 mg/ml	0.856	0.0055	0.1386	0.0397	1.31%
1 mg/ml	0.9308	0.0017	0.0675	0.0252	0.83%

TABLE II
Effect of Avemar on RNA ribose synthesis

Ribose isotopomers obtained from the experiment with glucose label are shown as *m0, m1, m2, m3,* and *m4*, which represent unlabeled, 1, 2, 3, and 4 ^{13}C substitutions assembled by specific synthesis pathways for nucleic acid ribose synthesis. Σm_n represents the molar enrichment of ^{13}C for each condition. S.E. in all cases was lower than 0.1% of the mean value.

Ribose	m0	m1	m2	m3	m4	Σm_n
Control	0.5536	0.1529	0.2209	0.0289	0.0457	0.8675
Avemar						
0.1 mg/ml	0.5765	0.1424	0.2139	0.0254	0.0415	0.8141
0.5 mg/ml	0.6275	0.1332	0.1844	0.0231	0.0315	0.6987
1 mg/ml	0.9308	0.0324	0.1125	0.0097	0.0094	0.3482

tumor cells' metabolic needs for reducing equivalents, which would intensively be used for the reduction of ribonucleotides to deoxyribonucleotides during DNA replication because Avemar inhibits key enzymes that are critically important both in nucleic acid ribose synthesis and fatty acid production. The reversion of transformed cell-specific metabolic changes that consist of increased glucose utilization for nucleic acid synthesis and proliferation (21, 29) has been shown to be an effective approach for developing new cancer therapies where natural products such as Avemar may play a key role as nutritional supplements with no know toxic effects.

The specific cancer fighting constituents of Avemar are not yet known. It is likely that multiple naturally produced compounds contained in the crude powder of fermented wheat germ induce the complex metabolic- and apoptosis-inducing effects inhibiting multiple tyrosine phosphorylase signaling cascades and the down-regulation of major histocompatibility complex I (MHC I) involved in immune protection, migration, tumor metastasis formation, and growth, as shown in other *in vitro* models of leukemia (30). Comparison of the anticancer metabolic effects of Avemar to that of the new effective anti-leukemia drug Gleevec reveals similarities in the metabolic enzyme and carbon substrate flow modifying effects toward nucleic acid synthesis. Gleevec inhibits glucose phosphorylation and oxidation in the oxidative branch of the pentose cycle, which is specific to inhibiting the tyrosine kinase activity of BCR-ABL in myeloid tumor cells (31, 32). Avemar has additional multiple effects on metabolic enzymes, and it simultaneously inhibits oxidative and nonoxidative ribose synthesis as well as the activation of glucose and glycolysis. Individual components of fermented wheat germ may be important anticancer natural drugs both as nutritional supplements and as therapeutic agents after they have been isolated and identified.

In conclusion, Avemar is a natural fermented wheat germ extract with no known toxicities, and it is a strong regulator of leukemia tumor cell macromolecule synthesis, cell cycle progression, apoptosis, and proliferation. Avemar regulates metabolic enzymes that are involved in glucose carbon redistribution between proliferation-related structural and functional macromolecules (RNA, DNA). Avemar treatment results in profound intracellular metabolic changes that bring devastating consequences for the proliferation of leukemia cells of the lymphoid lineage. Although the clinical applicability of Avemar together with current chemotherapies, surgical interventions, and radiation therapies has to be determined in controlled blinded clinical studies, this fermented wheat germ extract has a clear and definite anti-proliferative action that targets nucleic acid synthesis enzymes and induces cell cycle arrest and apoptosis through a caspase-based mechanism as reported herein.

REFERENCES

1. Reddy, B. S., Hirose, Y., Cohen, L. A., Simi, B., Cooma, I., and Rao, C. V. (2000) *Cancer Res.* **60,** 4792–4797
2. Zalatnai, A., Lapis, K., Szende, B., Raso, E., Telekes, A., Resetar, A., and Hidvegi, M. (2001) *Carcinogenesis* **22,** 1649–1652
3. Boros, L. G., Lapis, K., Szende, B., Tömösközi-Farkas, R., Balogh, A., Boren, J., Marin, S., Cascante, M., and Hidvegi, M. (2001) *Pancreas* **23,** 141–147, 201
4. Hidvégi, M., Ráso, E., Tömösközi-Farkas, R., Paku, S., Lapis, K., and Szende, B. (1998) *Anticancer Res.* **18,** 2353–2358
5. Hidvegi, M., Raso, E., Tomoskozi-Farkas, R., Lapis, K., and Szende, B. (1999) *Immunopharmacology* **41,** 183–186
6. Jakab, F., Mayer, Á., Hoffmann, A., and Hidvégi, M. (2000) *Hepatogastroenterology* **47,** 393–395
7. Jakab, F., Balogh, Á., Mayer, Á., Lapis, K., Hoffmann, A., Szentpétery, Á., Telekes, A., and Hidvégi, M. (2001) *Hepatogastroenterology* **48,** Suppl. I, (Abstr. CL)
8. Demidov, L. V., Manzjuk, L. V., Kharkevitch G. Y., Artamonova, E. V., and Pirogova, N. A. (2002) *18th UICC International Cancer Congress, Oslo, Norway, June 30-July 5, 2002,* Abstr. P868, Norwegian Cancer Society
9. Haridas, V., Higuchi, M., Jayatilake, G. S., Bailey, D., Mujoo, K., Blake, M. E., Arntzen, C. J., and Gutterman, J. U. (2001) *Proc. Natl. Acad. Sci. U. S. A.,* **98,** 5821–5826
10. Inayat-Hussain, S. H., Winski, S. L. & Ross, D. (2001) *Toxicol. Appl. Pharmacol.,* **175,** 95–103
11. Piqué, M., Barragán, M., Dalmau, M., Bellosido, B., Pons, G., and Gil, J. (2000) *FEBS Lett.* **480,** 193–196
12. Boyum, A. (1968) *Scand. J. Clin. Invest.* **21,** 51–62
13. Orosz, F., Comín, B., Raïs, B., Puigjaner, J., Kovács, J., Tárkányi, G., Ács, T., Keve, T., Cascante, M., and Ovádi, J. (1999) *Br. J. Cancer,* **79,** 1356–1365
14. Comin-Anduix, B., Agell, N., Bachs, O., Ovádi, J., and Cascante, M. (2001) *Mol. Pharmacol.* **60,** 1235–1242
15. Laemmli, U. K. (1970) *Nature,* **227,** 680–685
16. Taules, M., Rius, E., Talaya, D., López-Girona, A, Bachs, O., and Agell, N. (1998) *J. Biol. Chem.* **273,** 33279–33286
17. De La Haba, G., Leder, I. G., and Racker, E. (1955) *J. Biol. Chem.* **214,** 409–426
18. Tian, W. N., Pignatare, J. N., and Stanton, R. C. (1994) *J. Biol. Chem.* **269,** 14798–14805
19. Mommsen, T. P., French, C. J., and Hochanechka, P. W. (1980) *Can. J. Zool.* **58,** 1785–1799
20. Grossbard, L., and Schimke, R. T. (1966) *J. Biol. Chem.* **241,** 3546–3560
21. Boros, L. G., Cascante, M., and Paul Lee, W. N. (2002) *Drug Discovery Today* **7,** 364–372
22. Boros, L. G., Puigjaner, J., Cascante, M., Lee, W. N., Brandes, J. L., Bassilian, S., Yusuf, F. I., Williams, R. D., Muscarella, P., Melvin, W. S., and Schirmer,

W. J. (1997) *Cancer Res.* **57,** 4242–4248

23. Lee, W. N., Boros, L. G., Puigjaner, J., Bassilian, S., Lim, S., and Cascante, M. (1998) *Am. J. Physiol.* **274,** E843–851
24. Castaño, E., Dalmau, M., Barragán, M., Pueyo, G., Bartrons, R., and Gil, J. (1999) *Br. J. Cancer* **81,** 294–299
25. Patel, T., Gores, G. J., and Kaufmann, S. H. (1996) *FASEB J.* **10,** 587–597
26. Suttle, S., Stamato, T., Perez, M. L., and Biaglow, J. (2000) *Radiat. Res.* **153,** 781–787
27. Tian, W. N., Braunstein, L. D., Apse, K., Pang J., Rose, M., Tian, X., and Stanton, R. C. (1999) *Am. J. Physiol.* **276,** C1121–C1131
28. Van Engeland, M., Nieland, L. J., Ramaeekers, F. C. Schutte, B., and

Reutelingsperger, C. P. (1998) *Cytometry* **31,** 1–9

29. Cascante, M., Boros, L. G., Comin-Anduix, B., de Atauri, P., Centelles, J. J., and Lee, P. W. (2002) *Nat. Biotechnol.* **20,** 243–249
30. Fajka-Boja, R., Hidvegi, M., Shoenfeld, Y., Ion, G., Demydenko, D., Tomoskozi-Farkas, R., Vizler, C., Telekes, A., Resetar, A., and Monostori, E. (2002) *Int. J. Oncol.* **20,** 563–570
31. Boren, J., Cascante, M., Marin, S., Comin-Anduix, B., Centelles, J. J., Lim, S., Bassilian, S., Ahmed, S., Lee, W. N., and Boros, L. G. (2001) *J. Biol. Chem.* **276,** 37747–37753
32. Boros, L. G., Lee, W-N. P., and Cascante, M. (2002) *N. Engl. J. Med.* **347,** 67–68